

Infrared spectroscopic studies of hydrogenated silicon clusters

Guiding the search for Si_2H_x species in the Circumstellar Envelope of IRC+10216

R. I. Kaiser^{1,2} and Y. Osamura³

¹ Department of Chemistry, University of Hawai'i at Manoa, Honolulu, HI 96822, USA
e-mail: kaiser@gold.chem.hawaii.edu

² Department of Physics and Astronomy, The Open University, Milton Keynes MK7 6AA, UK

³ Department of Chemistry, Rikkyo University, 3-34-1 Nishi-ikebukuro, Tokyo 171-8501, Japan

Received 19 February 2004 / Accepted 8 November 2004

Abstract. Silicon-bearing species Si_2H_x ($x = 1-6$) are probable candidates in the circumstellar envelope of IRC+10216. We have observed several fundamentals of new silicon-containing radicals Si_2H_3 and Si_2H_5 in addition to the well-known Si_2H_4 and Si_2H_6 species from infrared spectroscopy in low temperature silane matrices at 10 K. Several infrared bands identify the Si_2H_x species and can be used to search for these molecules in the circumstellar envelope of IRC+10216. These infrared bands are confirmed by ab initio quantum chemical calculation as well as via corresponding infrared spectra detected for the deuterated species Si_2D_x .

Key words. molecular data – molecular processes – astrochemistry

1. Introduction

Since the pioneering detection of the silane molecule (SiH_4) in the circumstellar envelope of the carbon star IRC+10216 (CW Leo) (Barratt 1978; Goldhaber & Betz 1984), astronomers identified nine silicon-bearing molecules in the gas phase of cold molecular clouds, star-forming regions, and circumstellar envelopes of evolved carbon stars. These individual molecules can be arranged in four groups: simple diatomic molecules of the general chemical formula SiX (group 1), silicon carbides holding the generic composition SiC_n (group 2), and silicon cyanides (group 3). The diatomic species silicon carbide (SiC), silicon sulfide (SiS), and silicon nitride (SiN) are important constituents of the circumstellar envelope of CW Leo (Cernicharo et al. 1989; Speck et al. 1997; Bieging & Nguyen 1989; Turner 1992). The second group – the silicon carbides – contains three members, i.e. the cyclic, C_{2v} symmetric silicon dicarbide molecule, SiC_2 (Thaddeus et al. 1984; Sarre et al. 1996; Chandra & Sahu 1993; Gensheimer & Snyder 1997; Lloyd Evans et al. 2000), a polar, rhomboidal bicyclic SiC_3 species (McCarthy et al. 1999; Apponi et al. 1999), and a closed-shell linear chain molecule of the formula SiC_4 (Ohishi et al. 1989). Silicon carbide and silicon dicarbide have similar column densities, whereas the higher members silicon tricarbon (SiC_3) and silicon tetracarbide (SiC_4) are 200 times less abundant, with silicon tricarbon 50% more copious than silicon tetracarbide. The last group contains only one molecule, i.e. the linear SiCN species (silicon monocyanoide), which has

also been detected in the envelope of this carbon star (Guelin et al. 2000). It is important to stress that some molecules like SiS were also detected in vibrationally excited ($v = 1$) states (Turner 1987). Note that silicon monoxide (SiO) has only been observed in star forming regions such as Sagittarius B2 (Peng et al. 1995; Schilke et al. 1997) and to a lesser extent in cold molecular clouds (Ziurys et al. 1989), but not in circumstellar envelopes of carbon-rich stars; a possible formation route of silicon monoxide might involve barrier-less reactions with molecular oxygen and the hydroxyl radical (LePicard et al. 2001).

Silicon, which is – besides helium and neon – the fifth most abundant element in the interstellar medium with abundances of 3×10^{-5} relative to hydrogen, does not exist only in isolated gas phase molecules, but also as silicon-bearing nano particles – so-called dust grains – in circumstellar envelopes of late-type stars. As evident from the $11 \mu\text{m}$ emission feature, silicon subsists as silicon carbide nano particles in carbon-rich giants (Goebel et al. 1995; Blanco et al. 1998). Pillinger & Russel (1993) identified these silicon carbide particles also in meteorites; their role as cometary dust particles should be pointed out, too (Orofino et al. 1994). If the central star is oxygen-rich, silicates such as olivine ($(\text{Fe}, \text{Mg})_2\text{SiO}_4$) dominate their spectra (Fabian et al. 2001). Note that crystalline silicon nanoparticles might also explain the red emission as observed, for example, in the Red Rectangle (Ledoux et al. 2001). The assignment of silicon disulfide (SiS_2) as a carrier of the unidentified $21 \mu\text{m}$

emission feature must be regarded as tentatively (Kraus et al. 1997).

The abundances of these highly unsaturated, silicon-bearing molecules were first discussed in terms of $\text{Si}^+(\text{}^2\text{P}_j)$ -initiated ion-molecule reactions (Glassgold et al. 1986). This model has been expanded later by photon-induced reactions and photodissociation processes to account for the observation of the newly discovered SiC_3 and SiC_4 species (Glassgold & Mamon 1992; Howe & Millar 1994; Willacy & Cherchneff 1998) and for the abundances of silicon monoxide in interstellar clouds and in photon-dominated regions (Langer & Glassgold 1990; Walmsley et al. 1999). Also, Mackay (1995) investigated the chemistry of silicon in hot molecular cores, identifying silane as a reservoir for silicon. However, with the exception of silane, no hydrogenated, silicon-containing molecule has ever been observed in the interstellar medium.

From the astrochemical viewpoint, this is quite surprising. Recent laboratory experiments investigated the photochemistry of silane and the subsequent reactions of the photodissociation products. These data suggested that more complex, hydrogenated silicon clusters of the generic formula Si_2H_x ($x = 1-6$) are formed in these processes (Cook et al. 2001; Zavelovich & Lyman 1989; Hu et al. 2003; Glenewinkel-Meyer et al. 1993; Tonokura et al. 1992; Perkins et al. 1979; Borsella et al. 1988; Ashfold et al. 1996; Aka & Boch 2002; Wang & Huang 1998; Oikawa et al. 1994). Their experiments suggest that a rich silane chemistry is expected in the circumstellar envelope of IRC+10216: photochemistry of silane molecules close to the photosphere could contribute to the formation of small hydrogenated silicon clusters of the generic formula Si_2H_x . One drawback of astronomical observations are their vanishing (Si_2H_6) or relatively small dipole moments of less than 1.1 Debye. Therefore, an infrared spectroscopic search of the Si_2H_x species might present a viable alternative. To guide a search for hydrogenated silicon clusters in the circumstellar envelope of IRC+10216, we present in this paper a combined experimental and theoretical investigation of the infrared spectra and the vibronic levels together with their intensities of various Si_2H_x ($x = 1-6$) isomers. These data will assist a positive identification of hydrogen-rich silicon clusters in future infrared spectroscopic surveys of the circumstellar envelope of IRC+10216.

2. Computational approach

The molecular structures and vibrational frequencies of the Si_2H_x ($x = 1-6$) isomers and their fully deuterated counterparts were scrutinized in terms of ab initio molecular orbital methods. The geometries were optimized with the hybrid density functional method (B3LYP), i.e. Becke's three-parameter non-local exchange functional (Becke 1993) with the non-local correlation functional of Lee et al. (1988) and the 6-311G(d, p) basis set (Krishnan et al. 1980). Since the energies of the quartet electronic states of the Si_2H_x ($x = 1, 3, 5$) species and the triplet electronic states of the Si_2H_x ($x = 4, 6$) isomers are extremely high, we have only computed the doublet and singlet electronic states. To facilitate

spectroscopic identification in circumstellar envelopes, we also obtained vibrational frequencies and infrared intensities. The coupled cluster CCSD(T) calculations (Cizek 1969; Pople et al. 1987) with the aug-cc-pVTZ basis set (Kendall et al. 1992) were also performed at the optimized structures obtained with the B3LYP method. All computations were carried out using the GAUSSIAN 98 program package (Frisch et al. 2002). The relative energies stated in the text are the values obtained with the CCSD(T) method corrected with the zero-point vibrational energies obtained with the B3LYP method.

3. Experimental procedure

Our experiments were conducted in a contamination-free ultra-high vacuum (UHV) chamber which can be evacuated down to 2×10^{-10} torr by a magnetically suspended turbopump backed by an oil-free scroll pump. A rotatable, two-stage closed-cycle helium refrigerator is attached to the lid of the machine and holds a polished silver single crystal. This crystal is cooled to 10 K and serves as a substrate for the silane and d4-silane ices. The silane ices were prepared at 10 K by depositing silane (99.99%) and d4-silane (99.99%) at pressures of 6×10^{-8} torr for 30 min onto the cooled silver crystal. The absorptions of the silane and d4-silane samples are compiled in Table 1. To determine the ice thickness quantitatively, we integrated the infrared absorption features at 2163 cm^{-1} and 876 cm^{-1} and calculated the ice thickness via the Lambert-Beers relationship (Bennet et al. 2004). Considering the integrated absorption coefficients of these fundamentals, i.e. $2.5 \times 10^{-17} \text{ cm}$ and $2.0 \times 10^{-17} \text{ cm}$, and a density of the silane ice of $0.77 \pm 0.03 \text{ g cm}^{-3}$ (Sears & Morrison 1975), an optical thickness of $0.21 \pm 0.01 \mu\text{m}$ silane can be derived. We can compare our infrared spectra with literature data (Nucara et al. 1997; Calvani et al. 1990; Fournier et al. 1972). This suggests that the frozen high temperature modifications of $\text{SiH}_4(\text{I})$ and $\text{SiD}_4(\text{I})$ dominate the constitution of the sample. However, the presence of the ν_2 peak, which is infrared-inactive in crystalline $\text{SiH}_4(\text{I})$, suggests that the sample is partially disordered, possibly amorphous. We would like to point out that silane is certainly not a perfect matrix material to observe all fundamentals of the newly detected silicon-bearing molecules; smaller fundamentals can be obscured by the absorption of the parent molecules. Nevertheless, the detection of new silicon-containing molecules requires large concentrations of silicon-bearing reactant molecules, which is best achieved in pure silane and perdeutero-silane matrices.

The ices were irradiated at 10 K with 5 keV electrons generated in an electron gun at beam currents of 10 nA, 100 nA, and 1000 nA by scanning the electron beam over an area of $3.0 \pm 0.4 \text{ cm}^2$. We would like to stress that the electron beam is used to crack the silicon-hydrogen bonds – initially in the silane molecule and successively in higher order silicon-bearing molecules. The electron irradiation does not simulate the radiation environment around IRC+10216. Taking into account the irradiation times of between 10 and 120 min and the extraction efficiency of 78.8% of the electrons, this exposes the targets from 3.0×10^{13} to 4.5×10^{16} electrons. To guarantee an identification of the reaction products

Table 1. Infrared absorptions of the silane (left column) and d4-silane (center column) frosts (sh: shoulder); α , β , and γ denote lattice modes of the silane sample. The corresponding silane and d4-silane spectra are shown in Fig. 1.

Frequency, cm^{-1}	Frequency, cm^{-1}	Assignment
4354	3183	$2\nu_3$
4283	3128	$\nu_1 + \nu_3$
3142 (sh)	2264	$\nu_3 + \nu_4 + \beta$
3128	2243	$\nu_2 + \nu_3$
3087	2202	$\nu_3 + \nu_4 + \alpha$
3060	2173	$\nu_3 + \nu_4$
2300	1670	$\nu_3 + \gamma$
2250	1638	$\nu_3 + \beta$
2195	1607	$\nu_3 + \alpha$
2163	1581	ν_3
1876	1359	$\nu_2 + \nu_4 + \alpha$
1844	1334	$\nu_2 + \nu_4$
1050	781	$\nu_2 + \beta / \nu_4 + \gamma$
957	681	ν_2
948	703	$\nu_4 + \beta$
918	681	$\nu_4 + \alpha$
876	647	ν_4

in the ices and those sublimation into the gas phase on line and in situ, a Fourier transform infrared spectrometer (FTIR; solid state) and a quadrupole mass spectrometer (QMS; gas phase) were utilized. The Nicolet 510 DX FTIR spectrometer operates in an absorption-reflection-absorption mode (reflection angle ($\alpha = 75^\circ$) (resolution $0.5\text{--}2\text{ cm}^{-1}$; spectra were averaged for 180 s). The infrared beam is coupled via a mirror flipper outside the spectrometer, passes through a differentially pumped potassium bromide (KBr) window, is attenuated in the ice sample before and after reflection at a polished silver waver, and exits the main chamber through a second differentially pumped KBr window before being monitored via a liquid nitrogen cooled detector. The gas phase is monitored by a quadrupole mass spectrometer (Balzer QMG 420; $1\text{--}200\text{ amu}$ mass range) with electron impact ionization of the neutral molecules.

4. Results

The response of the irradiation of the silane system at 10 K is dictated by the initial appearance of the silyl radical, $\text{SiH}_3(X^2A_1)$. This species could be attributed to the 722 cm^{-1} band (Table 2, Figs. 1 and 2). The position of this ν_2 umbrella mode agrees well with earlier studies employing hydrogen and noble gas matrices ($721\text{--}738\text{ cm}^{-1}$) (Andrews & Wang 2002). A band at 820 cm^{-1} , which was assigned to the ν_6 fundamental of the disilane molecule, $\text{Si}_2\text{H}_6(X^1A_{1g})$ (Andrews & Wang 2002), appeared immediately at the beginning of the irradiation (Figs. 1 and 2, Table 3). Note that the less intense deformation mode of the SiH_3 group is observable at 935 cm^{-1} as a shoulder. We would like to stress that the assignments of all peaks were double checked in perdeuterated silane (SiD_4) matrices.

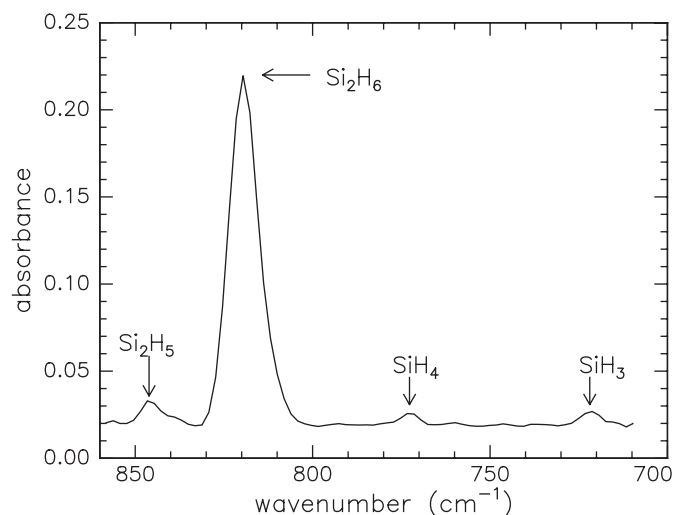


Fig. 1. Absorption of the newly synthesized silicon-bearing silyl radical (SiH_3) and disilane molecule (Si_2H_6).

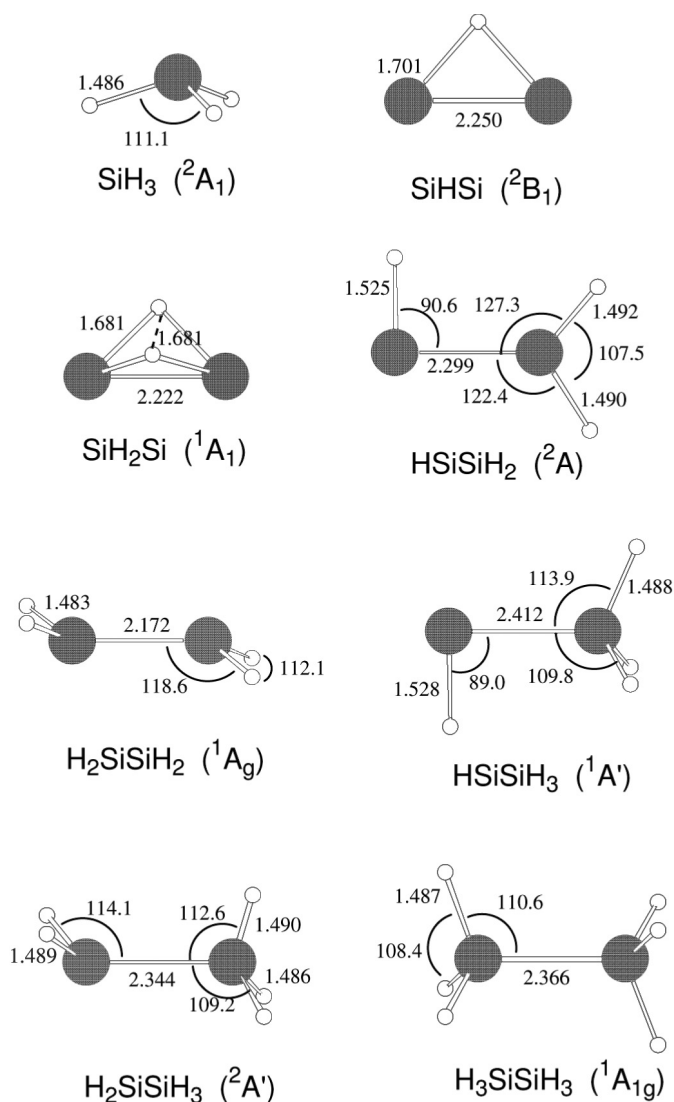


Fig. 2. Calculated structures of various SiH_3 and Si_2H_x ($x = 1\text{--}6$) species with the B3LYP methods. Bond lengths and bond angles are in Å and degrees.

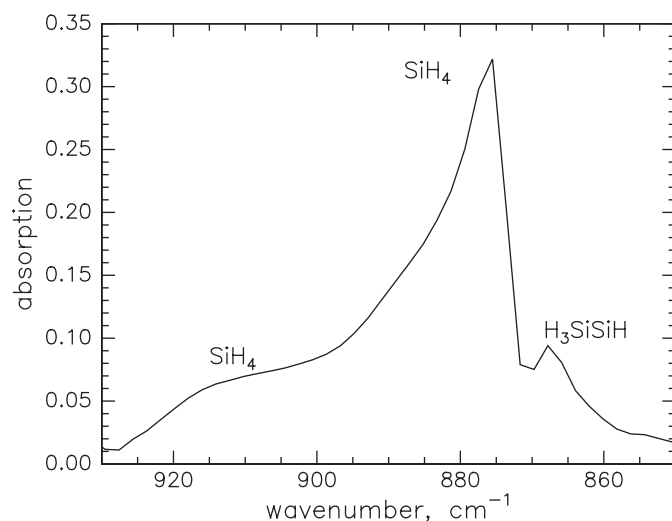
Table 2. Unscaled vibrational frequencies (cm^{-1}) and their infrared intensities (km mol^{-1}) of various SiH_n ($n = 1-3$) species calculated with B3LYP/6-311G(d, p) method. The deuterated species are included for completeness.

Mode	Characterization	Frequency	Intensity	Frequency	Intensity
		SiH($X^2\Pi$)		SiD($X^2\Pi$)	
σ_g	Stretching	2014	331	1449	171
		SiH ₂ (X^1A_1)		SiD ₂ (X^1A_1)	
a ₁	Symmetric stretching	2041	268	1467	145
a ₁	Bending	1024	93	736	46
b ₂	Asymmetric stretching	2039	302	1468	156
		SiH ₃ (X^2A_1)		SiD ₃ (X^2A_1)	
a ₁	Symmetric stretching	2193	5	1557	3
a ₁	Umbrella	760	77	561	42
e	Asymmetric stretching	2234	255	1616	143
e	Deformation	937	132	674	67

Here, we detected two fundamentals of the d3-silyl radical, $\text{SiD}_3(X^2A_1)$, at 669 cm^{-1} (ν_2) and 540 cm^{-1} (ν_4); this assignment corresponds very well with previously assigned peak positions at 668 cm^{-1} and about 546 cm^{-1} in noble gas matrices. Likewise, the d6-disilane molecule was detected in our experiments via its absorptions at 606 cm^{-1} (ν_6) and 1541 cm^{-1} (ν_5).

At longer irradiation times, we observed a new absorption at 843 cm^{-1} in the silane matrix (Fig. 1) and at 621 cm^{-1} in the perdeutero-silane matrix. We can now compare our calculated absorption frequencies with the experimentally observed ones (Table 3). Accounting for a scaling factor of 0.97 – a reasonable value for the B3LYP/6-311G(d,p) level of theory – the theoretical data predict that the most intense absorption of the disilyl radical (Fig. 2) should be observable at 849 cm^{-1} ($\text{Si}_2\text{H}_5(X^2A')$) and 621 cm^{-1} ($\text{Si}_2\text{D}_5(X^2A')$); these predictions are in excellent agreement with our observations. Note that this molecule has not been observed in the reaction of laser ablated silicon atoms in hydrogen matrices (Andrews & Wang 2002; Wang & Andrews 2003).

As the exposure time of the silane matrices increases even further, new bands appear at 867 cm^{-1} (silane matrix; Fig. 3) and 635 cm^{-1} (d4-silane matrix). A shoulder is also observable at 528 cm^{-1} in the d4-silane matrix. We then compared the observed absorptions with those computed for the three energetically most stable Si_2H_4 isomers – potential radiolysis products of the disilyl radical (Table 3). Both the 867 cm^{-1} and 635 cm^{-1} absorptions can be clearly assigned as the most intense ν_5 fundamental (umbrella mode of the $\text{SiH}_3/\text{SiD}_3$ group) of the $\text{H}_3\text{SiSiH}(X^1A')$ molecule and its d4-isotopomer. Scaling the computed data with a factor of 0.99 gives an excellent agreement with our experimental frequencies. We would like to stress that we were not able to detect any absorption of the thermodynamically more stable $\text{H}_2\text{SiSiH}_2(X^1A_g)$ isomer (Fig. 2). Our calculations suggest that the $\text{H}_2\text{SiSiH}_2(X^1A_g)$ structure is favorable by about 25 kJ mol^{-1} (27 kJ mol^{-1} is the value with CCSD(T) method) compared to $\text{H}_3\text{SiSiH}(X^1A')$. The reader should note that the most intense ν_{11} mode of $\text{H}_2\text{SiSiH}_2(X^1A_g)$ falls within the ν_4 and $\nu_4 + \alpha$ absorptions of the silane matrix (Table 1). We would like to stress that Andrews & Wang (2002) also identified a Si_2H_4 species in hydrogen matrices,

**Fig. 3.** New absorption features of the silylsilylene (HSiSiH_3, X^1A') isomer at 867 cm^{-1} in the silane matrix at 10 K; the ν_4 fundamental (876 cm^{-1}) and the $\nu_4 + \alpha$ combination bands (918 cm^{-1}) of the silane matrix are also shown.

but no compelling assignment of the isomer was presented. Comparing their data of 861.4 cm^{-1} (hydrogen in neon) and 634.2 cm^{-1} (deuterium in neon), we suggest that they observed the $\text{H}_3\text{SiSiH}(X^1A')$ structure. We would like to point out that Maier et al. (2002) observed this isomer, too. Their strongest absorptions at 860.6 cm^{-1} and 642.4 cm^{-1} are very close to our experimentally observed value of 867 cm^{-1} and 635 cm^{-1} . The less intense peaks are hidden by the silane matrices.

With an enhanced electron exposure, additional bands at 651 cm^{-1} (Fig. 4; silane target) as well as 493 cm^{-1} and 683 cm^{-1} (d4-silane) appeared. These lines cannot be attributed to any $\text{Si}_2\text{H}_x/\text{Si}_2\text{D}_x$ ($x = 4-6$) isomer. We matched these data with the energetically most stable $\text{Si}_2\text{H}_3/\text{Si}_2\text{D}_3$ structures – suggesting that the newly observed bands originate from an electron-induced decomposition of the $\text{Si}_2\text{H}_4/\text{Si}_2\text{D}_4$ isomers. Indeed, we verified the existence of the $\text{H}_2\text{SiSiH}(X^2A)$ isomer and also its perdeuterated isotopomers via the ν_5 (rocking) and ν_4 (scissoring of H_2Si part; shoulder) fundamentals.

Table 3. Unscaled vibrational frequencies (cm^{-1}) and their infrared intensities (km mol^{-1}) of Si_2H_x and Si_2D_x species ($x = 1-6$) calculated with B3LYP/6-311G(d, p) method.

Mode	Characterization	Frequency	Intensity	Frequency	Intensity
		H_3SiSiH_3		D_3SiSiD_3	
$\nu_1(a_{1g})$	Symmetric stretch	2219	0	1580	0
$\nu_2(a_{1g})$	Deformation	927	0	694	0
$\nu_3(a_{1g})$	Si-Si stretching	421	0	396	0
$\nu_4(a_{1u})$	Torsion	135	0	96	0
$\nu_5(a_{2u})$	Symmetric stretch	2210	122	1572	71
$\nu_6(a_{2u})$	Deformation	854	546	630	295
$\nu_7(e_g)$	Stretching	2220	0	1604	0
$\nu_8(e_g)$	Deformation	945	0	675	0
$\nu_9(e_g)$	Rocking	636	0	484	0
$\nu_{10}(e_u)$	Stretching	2230	208	1612	118
$\nu_{11}(e_u)$	Deformation	960	92	689	48
$\nu_{12}(e_u)$	Rocking	381	27	272	13
		H_3SiSiH_2		D_3SiSiD_2	
$\nu_1(a')$	SiH_3 antisymmetric stretch	2223	75	1600	56
$\nu_2(a')$	Symmetric stretch	2199	72	1571	15
$\nu_3(a')$	Symmetric stretch	2188	101	1564	70
$\nu_4(a')$	Umbrella	949	63	691	20
$\nu_5(a')$	Bending	936	2	676	16
$\nu_6(a')$	Umbrella	875	420	641	223
$\nu_7(a')$	Rocking	596	18	454	10
$\nu_8(a')$	Si-Si stretching	424	3	403	0
$\nu_9(a')$	Rocking	405	20	294	11
$\nu_{10}(a'')$	SiH_3 antisymmetric stretching	2231	158	1613	93
$\nu_{11}(a'')$	SiH_2 antisymmetric stretching	2213	48	1600	20
$\nu_{12}(a'')$	Deformation	950	44	680	23
$\nu_{13}(a'')$	Deformation	637	1	481	0
$\nu_{14}(a'')$	Deformation	390	21	278	10
$\nu_{15}(a'')$	Torsion	127	0	91	0
		H_2SiSiH_2		D_2SiSiD_2	
$\nu_1(a_g)$	Symmetric SiH stretch	2229	0	1596	0
$\nu_2(a_g)$	Symmetric SiH_2 bend	956	0	713	0
$\nu_3(a_g)$	Si-Si stretch	562	0	614	0
$\nu_4(a_g)$	Rocking	324	0	254	0
$\nu_5(a_u)$	Asymmetric SiH stretch	2258	148	1634	79
$\nu_6(a_u)$	Torsion	525	0	371	0
$\nu_7(a_u)$	Deformation	348	23	249	12
$\nu_8(b_g)$	Asymmetric SiH stretch	2246	0	1625	0
$\nu_9(b_g)$	Deformation	616	0	469	0
$\nu_{10}(b_u)$	Symmetric SiH stretch	2225	110	1590	61
$\nu_{11}(b_u)$	Symmetric SiH_2 bend	920	183	665	95
$\nu_{12}(b_u)$	Rocking	447	32	327	17
		H_3SiSiH		D_3SiSiD	
$\nu_1(a')$	SiH stretching	2214	128	1597	75
$\nu_2(a')$	Symmetric SiH stretching	2179	76	1553	40
$\nu_3(a')$	SiH stretching	2037	206	1465	106
$\nu_4(a')$	SiH_3 deformation	933	71	671	60
$\nu_5(a')$	SiH_3 umbrella	868	222	641	78
$\nu_6(a')$	SiH bending	716	62	533	42
$\nu_7(a')$	Rocking	426	24	377	16
$\nu_8(a')$	Si-Si stretching	368	8	288	9
$\nu_9(a'')$	Asymmetric SiH stretching	2188	109	1580	63
$\nu_{10}(a'')$	SiH_3 deformation	957	38	686	21
$\nu_{11}(a'')$	Deformation	386	29	280	15
$\nu_{12}(a'')$	Torsion	51	10	37	5
		H_2SiSiH		D_2SiSiD	
$\nu_1(a)$	Asymmetric Si-H stretch	2210	121	1596	68
$\nu_2(a)$	Symmetric Si-H stretch	2180	109	1562	57
$\nu_3(a)$	Si-H stretch	2041	182	1468	92
$\nu_4(a)$	SiH_2 scissor	965	93	702	42
$\nu_5(a)$	Rocking	683	24	511	18
$\nu_6(a)$	Deformation	448	6	422	7
$\nu_7(a)$	Out-of-plane	402	9	298	4
$\nu_8(a)$	Deformation	385	13	279	7
$\nu_9(a)$	Torsion	192	7	142	4
		SiH_2Si		SiD_2Si	
$\nu_1(a_1)$	Symmetric H stretch	1615	9	1150	5
$\nu_2(a_1)$	Asymmetric H stretch	963	54	712	25
$\nu_3(a_1)$	Si-Si stretch	522	1	505	3
$\nu_4(a_2)$	Asymmetric H-shift	1082	0	776	0
$\nu_5(b_1)$	Asymmetric H deform	1533	21	1096	11
$\nu_6(b_1)$	Symmetric H-shift	1174	372	852	195
		SiHSi		SiDSi	
$\nu_1(a_1)$	Sym H stretch	1476	41	1057	21
$\nu_2(a_1)$	Si-Si stretch	509	0	507	0
$\nu_3(b_2)$	H shift	1035	129	746	67

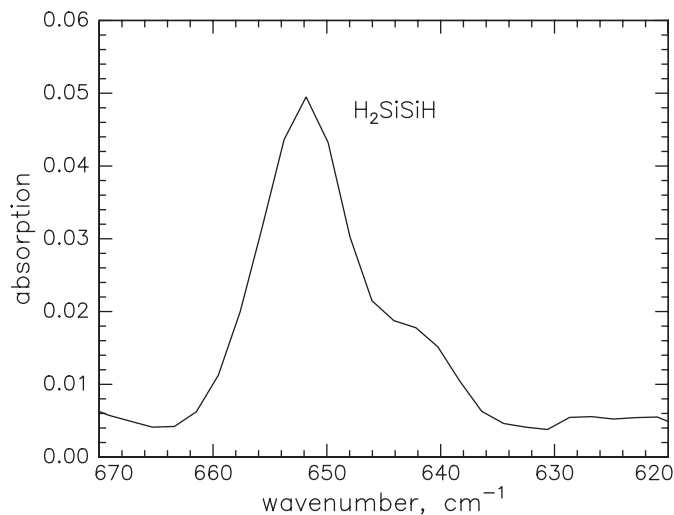


Fig. 4. New absorption features of the silylsilylenyl radical (HSiSiH_2 , X^2A) isomer at 651 cm^{-1} in the silane matrix at 10 K.

Table 4. Compilation of newly observed hydrogenated silicon-bearing molecules and their absorptions.

Species	Frequency, cm^{-1}	Fundamental
SiH_3	722	ν_2
Si_2H_6	820	ν_6
	935	ν_8
Si_2H_5	843	ν_6
H_3SiSiH	867	ν_5
H_2SiSiH_2	898	ν_{11}
H_2SiSiH	651	ν_5

A scaling factor of about 0.97 converts the calculated absorptions into the experimentally observed lines. For $\text{H}_2\text{SiSiH}(X^2A)$, the more intense ν_1 – ν_4 modes overlap with those of the silane molecule. Compared to the estimation by Sari et al. (2003), which suggested that the bridged $\text{H}_2\text{SiHSi}(X^2A)$ isomer is the energetically most stable one followed by $\text{H}_2\text{SiSiH}(X^2A)$ ($+1\text{ kJ mol}^{-1}$) and $\text{H}_3\text{SiSi}(X^2A)$ ($+13\text{ kJ mol}^{-1}$), our calculation leads to the conclusion that all three isomers lie within 0.5 kJ mol^{-1} . We were not able to detect any absorption of any Si_2H_2 isomers.

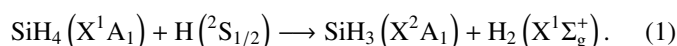
After the experiment, the silane sample was heated at a rate of 0.5 K min^{-1} to 293 K. After the sublimation of the silane matrix at 80 K, we observed additional peaks at 898 cm^{-1} (silane experiment) and 658 cm^{-1} (d4-silane experiment). These lines were compared with Table 3. Here, we identified the 898 cm^{-1} and 658 cm^{-1} absorptions as the most intense ν_{11} (symmetric $\text{SiH}_2/\text{SiD}_2$ bending) fundamental of the thermodynamically most stable $\text{H}_2\text{SiSiH}_2(X^1A_g)$ isomer and its perdeuterated counterpart (Fig. 2, Table 4). It is important to compare our findings with an earlier study of Maier et al. (2002). Here, the authors observed the strongest absorption at 904.3 cm^{-1} close to our observed fundamental at 898 cm^{-1} ; two weak silicon-hydrogen stretching modes at 2180.2 cm^{-1} and 2207.8 cm^{-1} are obscured in our silane matrix.

Table 5. Calculated dipole moments and rotational constants for SiH_x ($x = 1$ –3) and Si_2H_x ($x = 1$ –6) species obtained with the B3LYP method.

	Dipole moment		Rotational constants	
	(debye)		(GHz)	
SiH	0.13	0.00	220.37	220.37
SiH_2	0.15	236.51	209.18	110.99
SiH_3	0.20	140.81	140.81	83.44
SiHSi	0.43	313.40	7.13	6.98
SiH_2Si	0.36	159.56	7.20	7.12
HSiSiH_2	0.89	96.15	6.05	5.72
H_2SiSiH_2	0	75.38	6.34	5.93
HSiSiH_3	0.30	62.33	5.34	5.21
H_2SiSiH_3	0.11	53.05	5.29	5.17
H_3SiSiH_3	0	43.00	5.01	5.01

5. Astrophysical implications

Our combined experimental and theoretical investigations provide reliable infrared absorptions and their intensities of astrophysically important hydrogenated, silicon-bearing molecules (Table 4); all assignments were carefully verified in d4-silane matrices. Two classes of molecules could be identified from the present laboratory study. These are SiH_x species ($x = 1$ –3) and Si_2H_x ($x = 1$ –6). The ν_2 fundamental of the silyl radical (SiH_3 ; 722 cm^{-1}) can be detected easily in future infrared spectroscopic studies of the circumstellar envelope of IRC+10216. Although photodissociation of silane molecules preferentially yields the $\text{SiH}_2(X^1A_1)$ and $\text{SiH}(X^2\Pi)$ species, whose infrared absorptions can be found in Table 2, reactions of photolytically generated, suprathermal hydrogen atoms with silane can actually yield the silyl radical via a direct abstraction reaction (Eq. (1)):



Note that the corresponding methyl radical, $\text{CH}_3(X^2A_1)$, has been observed in the atmospheres of the giant planets Saturn (Atreya et al. 1999; Bezdard et al. 1999) and Neptune (Bezdard et al. 1998; Lee et al. 2000) utilizing the Infrared Space Observatory (ISO). Only upper limits have been derived for Jupiter, Uranus, and Titan (Lee et al. 2000; Atreya et al. 2003). The methyl radical has also been detected in the interstellar medium toward the Galactic Center Sagittarius A via the ν_2 Q-branch at $16.5\text{ }\mu\text{m}$ and the R(0) line at $16.0\text{ }\mu\text{m}$ with abundances of $1.3 \pm 0.7 \times 10^{-8}$ relative to hydrogen (Feuchthuber et al. 2000), too. However, the silane species and the corresponding silyl radical have eluded a positive identification in the atmospheres of any solar system body so far; only upper limits of silane in Saturn have been published (Larson et al. 1980).

Considering the Si_2H_x ($x = 1$ –6) and the homologues C_2H_x ($x = 1$ –6) series, we would like to stress that silicon-bearing species have been detected neither in the solar system nor in the interstellar medium. On the other hand,

members of the homologues C_2H_x ($x = 1-6$) series are ubiquitous in extraterrestrial environments. Here, ethane (C_2H_6) and acetylene (C_2H_2) are actually present in the atmospheres of the giant planets Jupiter and Saturn (Fouchet et al. 1999; Courtin et al. 1984) as well as Uranus (Atreya et al. 1999; Bishop et al. 1990) and Neptune (Conrath et al. 1989; Orton et al. 1992). Ethylene (C_2H_4) was only observed in Jupiter and Neptune (Encrenaz et al. 2002; Fegley 1995). Ethane has also been identified in comets such as 153P/Ikeya-Zhang (Kawakita et al. 2003). Note that ethylene (Goldhaber et al. 1987), acetylene (Cernicharo et al. 1999), and the ethynyl radical (Fuente et al. 1998) have been detected in the circumstellar envelope of IRC+10216. Our studies provide solid data for a prospective infrared spectroscopic search Si_2H_x ($x = 1-6$), preferentially in the 600–800 cm^{-1} range (16.6–12.5 μm ; Tables 3 and 4). These investigations should also help to elucidate the hitherto poorly understood organo-silicon chemistry in circumstellar envelopes of carbon-rich, dying stars.

Acknowledgements. The experiments were supported by the University of Hawai'i at Manoa (R.I.K.), by the Particle Physics and Astronomy Research Council (PPARC, UK) (R.I.K.), and by Osaka Vacuum (Japan) (R.I.K.). The computations were carried out at the Research Center for Computational Science, Japan, and supported by the Grants-in-Aid for Scientific Research on Priority Areas from the Ministry of Education, Science, and Culture, Japan (Y.O.).

References

- Aka, B., & Boch, E. J. 2002, *Photochem. Photobiol. A*, 150, 257
 Andrews, L., & Wang, W. 2002, *J. Phys. Chem. A*, 106, 7696
 Apponi, A. J., McCarthy, M. C., Gottlieb, C. A., & Thaddeus, P. 1999, *ApJ*, 516, L103
 Ashfold, M. N. R., Mordaunt, D. H., & Wilson, S. H. S. 1996, *Adv. Photochem.*, 21, 217
 Atreya, S. K., Edgington, S. G., Encrenaz, Th., & Feuchtgruber, H. 1999, *European Space Agency (Special Publication) SP*, 149
 Atreya, S. K., Mahaffy, P. R., Niemann, H. B., Wong, M. H., & Owen, T. C. 2003, *Planetary and Space Science*, 51, 105
 Barratt, A. 1978, *ApJ*, 220, L81
 Becke, A. D. 1993, *J. Chem. Phys.*, 98, 5648
 Bennett, C., Jamieson, C., Mebel, A. M., & Kaiser, R. I. 2004, *Phys. Chem. Chem. Phys.*, 6, 735
 Bezar, B., Feuchtgruber, H., Moses, J. I., & Encrenaz, T. 1998, *A&A*, 334, L41
 Bezar, B., Romani, P. N., Feuchtgruber, H., & Encrenaz, T. 1999, *ApJ*, 515, 868
 Biegging, J. H., & Nguyen, Q. R. 1989, *ApJ*, 343, L25
 Bishop, J., Atreya, S. K., Herbert, F., & Romani, P. 1990, *Icarus*, 88, 448
 Blanco, A., Birghesi, A., Fonti, S., & Orofino, V. 1998, *A&A*, 330, 505
 Borsella, E., & Fantoni, R. 1988, *Chem. Phys. Lett.*, 150, 542
 Calvani, P., Ciotti, C., Cunsolo, S., & Lupi, S. 1990, *Solid State Commun.*, 75, 189
 Cernicharo, J., Gottlieb, C. A., Guelin, M., Thaddeus, P., & Vrtilik, J. M. 1989, *ApJ*, 341, L25
 Cernicharo, J., Yamamura, I., Gonzalez-Alfonso, E. G., et al. 1999, *ApJ*, 526, L41
 Chandra, S., & Sahu, A. 1993, *A&A*, 272, 700
 Cizek, J. 1969, *Adv. Chem. Phys.*, 14, 35
 Conrath, B., et al. 1989, *Science*, 246, 1454
 Cook, P. A., Ashfold, M. N. R., Jee, Y.-J., et al. 2001, *Phys. Chem. Chem. Phys.*, 3, 1848
 Courtin, R., Gautier, D., Marten, A., Bezar, B., & Hanel, R. 1984, *ApJ*, 287, 899
 Encrenaz, Th. 2002, *Adv. Space Res.*, 30, 1967
 Fabian, D., Henning, T., Jager, C., et al. 2001, *A&A*, 378, 228
 Fegley, B. 1995, in *AGU Handbook of Physics Constants*, ed. T. Ahrens, 320
 Feuchtgruber, H., Helmich, F. P., Van Dishoeck, E. F., & Wright, C. M. 2000, *ApJ*, 535, L111
 Fouchet, Th., Lellouch, E., Encrenaz, Th., et al. 1999, *European Space Agency*, 177
 Fournier, R. P., The, N. D., Savoie, R., Belzile, R., & Cabana, A. 1972, *Can. J. Chem.*, 50, 35
 Frisch, M. J., et al. 2002, *GAUSSIAN98 Revision A11*, Gaussian, Inc.: Pittsburgh, P. A.
 Fuente, A., Cernicharo, J., & Omont, A. 1998, *A&A*, 330, 232
 Gensheimer, P. D., & Snyder, L. E. 1997, *ApJ*, 490, 819
 Glassgold, A. E., & Mamon, G. A. 1992, in *Chemistry and Spectroscopy of Interstellar Molecules*, ed. D. K. Bohme et al. (University of Tokyo Press), 261
 Glassgold, A. E., Lucas, R., & Omont, A. 1986, *A&A*, 157, 35
 Glenewinkel-Meyer, Th., Bartz, J. A., Thorson, G. M., & Crim, F. F. 1993, *J. Chem. Phys.*, 99, 5944
 Goebel, J. H., Cheeseman, P., & Gerbaullt, F. 1995, *ApJ*, 246, 246
 Goldhaber, D. M., & Betz, A. L. 1984, *ApJ*, 279, L55
 Goldhaber, D. M., Betz, A. L., & Ottusch, J. J. 1987, *ApJ*, 314, 356
 Guelin, M., Muller, S., Cernicharo, J., et al. 2000, *A&A*, 363, L9
 Howe, D. A., & Millar, T. J. 1990, *MNRAS*, 244, 444
 Hu, S.-W., Wang, Y., Wang, X.-Y., Chu, T.-W., & Liu, X.-Q. 2003, *J. Phys. Chem. A*, 107, 2954
 Kawakita, H., Watanabe, J., Kinoshita, D., Ishiguro, M., & Nakamura, R. 2003, *ApJ*, 590, 573
 Kendall, R. A., Dunning, T. H., & Harrison, R. J. 1992, *J. Chem. Phys.*, 96, 6796
 Kraus, G. D., Nuth, J. A., & Nelson, R. N. 1997, *A&A*, 328, 328
 Krishnan, R., Binkley, J. S., Seeger, R., & Pople, J. A. 1980, *Chem. Phys.*, 72, 650
 Langer, W. D., & Glassgold, A. E. 1990, *ApJ*, 352, 123
 Larson, H. P., Fink, U., Smith, H. A., & Davis, D. S. 1980, *ApJ*, 240, 327
 Le Picard, S. D., Canosa, A., Pineau des Forets, G., Rebrion-Rowe, C., & Rowe, B. R. 2001, *A&A*, 372, 1064
 Ledoux, G., Guillois, O., Huisken, F., et al. 2001, *A&A*, 377, 707
 Lee, A. Y. T., Yung, Y. L., & Moses, J. 2000, *J. Geophys. Res.*, 105, 20207
 Lee, C., Yang, W., & Parr, R. G. 1988, *Phys. Rev. B*, 37, 785
 Lloyd Evans, T., Hurst, M. E., & Sarre, P. J. 2000, *MNRAS*, 319, 111
 Mackay, D. D. S. 1995, *Ap&SS*, 224, 507
 Maier, G., Reisenauer, H. P., & Glatthaar, J. 2002, *Chem. Eur. J.*, 8, 4383
 McCarthy, M. C., Apponi, A. J., & Thaddeus, P. 1999, *J. Chem. Phys.*, 110, 10645
 Nucara, A., Calvani, P., Lupi, S., & Roy, P. 1997, *J. Chem. Phys.*, 107, 6562
 Ohishi, M., Kaifu, N., Kawaguchi, K., et al. 1989, *ApJ*, 345, L83
 Oikawa, S., Tsuda, M., & Ohtsuka, S. 1994, *J. Mol. Structure*, 310, 287
 Orofino, V., Blanco, A., & Fonti, S. 1994, *A&A*, 282, 657
 Orton, G., Lacy, J. H., Achtermann, J. M., Parmar, P., & Blass, W. E. 1992, *Icarus*, 100, 541

- Peng, Y., Vogel, S. N., & Carlstrom, J. E. 1995, *ApJ*, 455, 223
- Perkins, G. G. A., Austin, E. R., & Lampe, R. W. 1979, *J. Am. Chem. Soc.*, 101, 1109
- Pillinger, C. T., & Russel, S. 1993, *J. Chem. Soc. Faraday Trans.*, 89, 2297
- Pople, J. A., Head-Gordon, M., & Raghavachari, K. J. 1987, *Chem. Phys.*, 87, 5968
- Sari, L., McCarthy, M. C., Schaefer III, H. F., & Thaddeus, P. 2003, *J. Am. Chem. Soc.*, 125, 11409
- Sarre, P. J., Hurst, M. E., & Evans, T. L. 1996, *ApJ*, 471, L107
- Schilke, P., Walmsley, C. M., Pineau des Forets, G., & Flower, D. R. 1997, *A&A*, 321, 293
- Sears, W. M., & Morrison, J. A. 1975, *J. Chem. Phys.*, 62, 2736
- Speck, A. K., Barlow, M. J., & Skinner, C. J. 1997, *MNRAS*, 288, 431
- Thaddeus, P., Cummins, S. E., & Linka, R. A. 1984, *ApJ*, 283, L45
- Tonokuna, K., Mo, Y., Matsumi, Y., & Kawasaki, M. 1992, *J. Phys. Chem.*, 96, 6688
- Turner, B. E. 1987, *A&A*, 183, L23
- Turner, B. E. 1992, *ApJ*, 388, L35
- Walmsley, C. M., Pineau des Forets, G., & Flower, D. R. 1999, *A&A*, 342, 542
- Wang, X., & Andrews, L. 2003, *J. Am. Chem. Soc.*, 125, 6581
- Wang, Z. X., & Huang, M. B. 1998, *J. Chem. Soc. Faraday Trans.*, 94, 635
- Willacy, K., & Cherchneff, I. 1998, *A&A*, 330, 676
- Zavelovich, J., & Lyman, J. L. 1989, *J. Phys. Chem.*, 93, 5740
- Ziurys, L. M., Friberg, P., & Irvine, W. M. 1989, *ApJ*, 343, 201